View metadata, citation and similar papers at core.ac.uk

brought to you by CORE

J. TUŠEK, A. LEŠNJAK, M. PLETERSKI, D. KLOBČAR

ISSN 0543-5846
METABK 51(2) 175-178 (2012)
UDC – UDK 621.791.754:669.15-194.57:544.22=111

THE WELD-POOL SOLIDIFICATION MODE OF FERRITIC STAINLESS STEELS

Recevied – Prispjelo: 2011-01-14
Acctepted – Prihvaćeno: 2011-02-30
Original Scientific Paper – Izvorni znanstveni rad

The paper presents the analysis of solidification mode at gas tungsten arc welding (GTAW) of AISI 430 ferritic stainless steel. Two solidification modes (epitaxial and equiaxial) were discovered, which have a major influence on a weld tensile strength. The optimal welding parameters for ferritic stainless steels were found in a narrow range. They should be selected according to mechanical strength of the welded joints and not only according to their visual appearance.

Key words: ferritic stainless steel, grain growth, epitaxial, equaxial, GTAW

Utjecaj parametara zavarivanja na skrućivanje zavara kod feritnog nehrđajućeg čelika. U radu je prikazana analiza skrućivanja zavara kod TIG zavarivanja AISI 430 feritnog nehrđajućeg čelika. Dva načina skrućivanja bila su zapažena (epitaxial i equiaxial). Optimalni parametri zavarivanja su utvrđeni u uskome području. Odabir treba biti prema čvrstoći spojeva, a ne samo prema izgledu.

Ključne riječi: feritni nerđajući čelik, rast kristala, epitaxial, equaxial, TIG zavarivanje

INTRODUCTION

Ferritic stainless steels (FSS) are used as material for production of home appliances, furniture, laboratory equipment, where the material does not come into the contact with the aggressive media and where welded joints are not dynamically loaded. The FSS have a ferritic structure during solidification without any transformation in the entire temperature range. These steels are considered as difficult-to-weld due to their grain growth. The FSS are being replaced by expensive austenitic stainless steel, due to their good weldability. There is no need to replace FSS with the austenitic stainless steels if the appropriate welding parameters are used.

Two weld pool solidification modes (WPSM) of FSS are known i.e. (1) epitaxial and (2) equiaxial (Figure 1) [1,2]. At both solidification modes weld pool solidifies heterogeneously, by wetting the wall grains of the solid base metal. It is inferred that this is the beginning of the grain growth and that the size of the nucleus depends on the structure of the solid base metal. At epitaxial weld solidification mode, the grains grow from both sides of the base metal in direction to the weld-metal centre (Figure 1a). At equiaxial mode, a layer of independent grains is additionally formed in the middle of the weld pool, to which the grains from both sides of the base metal grow and meet (Figure 1b) [1,2].

The solidification of metals without transformation was at the beginning studied at gravity die casting of ferritic steels, titanium and especially aluminium alloys [3-5]. Hunt was the first to physically explain the equiaxial solidification using an assessment equation [6]. Easterling [7] discovered that intermediate grains in the weld metal occur only at higher welding speed. Clarc et al. [8] developed a model for prediction of formation of independent grains in the intermediate layer in the weld centre, based particularly on the chemical composition. They conducted the experiments at welding an alloy of aluminium and copper with the addition of titanium boride. An epitaxial and equiaxial weld-metal solidifications mode was theoretically and mathematically explained by Grong [9]. Hornbogen [10] studied the influence of alloying elements on the weld pool solidification mode at aluminium alloys. Kou et al. [11] described the weld pool solidification mode in aluminium alloy as a function of the energy input and welding speed. They presented three different weld metal solidification modes. Huang et al. [12] described the phenomena of the grain growth initiation in detail. The weld-pool solidification in welding of FSS studied Villafuerte et al. [13,14]. Witke [15-17] described the mode of solidification, the grain growth in the weld-pool solidification, and the solidification by equations and partial modelling of individual solidification processes. Eichorn [18] and Markelj et al. [19] explained the two modes of the weld-pool solidification in detail. They discovered that the solidification mode depends on the welding parameters, the material, and the workpiece thickness. The mode of solidification in relation to crack formation in a weld was treated by Katayama [20].

The results show that the size, shape, number, orientation and location of growth initiation of the grains were also influenced by the welding parameters and the chemical composition of FSS as well as by the shielding medium. The welding current and speed are the most influ-

J. Tušek, D. Klobčar, M. Pleterski, Faculty of Mechanical Engineering, University of Ljubljana, Ljubljana, Slovenia, A. Lešnjak, QTechna, Ljubljana, Slovenia

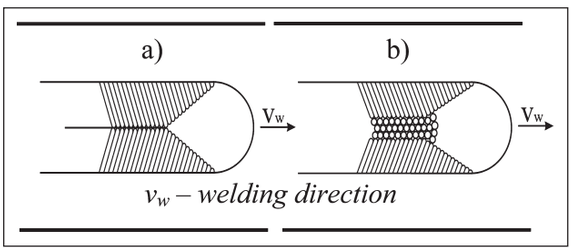

Figure 1 Weld pool solidification mode: a) epitaxial and b) equaxial

ential welding parameters. The weld pool solidification mode has a major influence on the weld strength.

EXPERIMENTAL WORK

Material

For GTAW experiments a 1.4016 (X 6 Cr 17) (AISI 430) FSS was used with the measured chemical composition: 0,055 % C; 16,5 % Cr; 0,75 % Si; 0,79 % Mn; 0,15 % Ni; 0,029 % P; 0,002 % S and the rest Fe. The workpiece dimensions were 250×90×1 mm (Figure 2). From the welded workpiece, a specimen for a micro and macro analysis (Figure 2-1) and tensile tests (Figure 2-2) were taken. Welds welded with the optimum welding parameters were tested for strength and metallurgical analysed.

GTA welding

A GTA welding of a butt welded joint (BWJ) was done without the filler material. Argon with a 5% addition of hydrogen was used as a shielding gas. Classical welding power source with a falling static characteristic and a water-cooled torch, connected to the minus pole of the power source was used. The torch was mounted on a carriage for automatic displacement during welding. A thoriated tungsten electrode of 2 mm in diameter was used. BWJ were welded on a 1 mm thick sheet (Figure 2) without the edge preparation. The experimental setup is shown in Figure 3.

The optimum welding parameters were determined at practical welding of a BWJ without a gap in the flat posi-

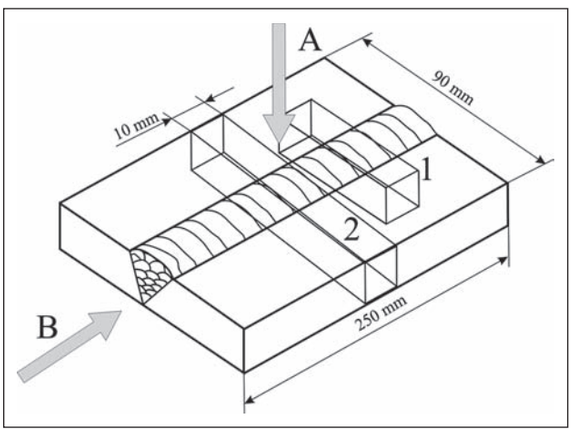

Figure 2 A butt welded joint; (1) specimen for micro and macro analysis, (2) tensile test specimen, (A) top view and (B) side view in the transverse direction to welding direction

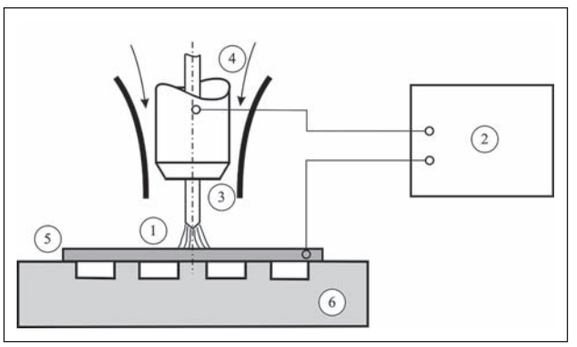

Figure 3 Experimental setup: 1 – arc, 2 – power source, 3 – W-electrode, 4 – shielding gas, 5 – workpiece, 6 – welding table

tion. Welding parameters were carefully chosen based on experience and literature data [19]. The welding current, arc voltage, welding speed, and arc length that exert the strongest influence on the shape, size and visual appearance of the weld, were carefully optimized. The shielding-gas flow rate was optimized according to welding current in a range between 4 and 7 l/min. The distance between the tungsten electrode tip and the workpiece ranged between 1,75 and 2,68 mm. It was in an almost linear relationship to the arc voltage. The arc voltage was thus predetermined by the arc length and was not optimized.

RESULTS AND DISSCUSION

The welds obtained by changing the welding current and speed were analysed according to weld appearance. A smooth weld face appearance without undercuts and with a good root penetration was found at welding parameters between minimum and maximum curve on Figure 4. Results of tensile test showed a much narrower range of the optimum welding parameters (Figure 4).

An analysis of macrographs of the BWJ showed two weld pool solidification modes (Figure 5A and 5C). Figure 5A shows top and side view of weld macrograph welded with 40 A at 0,31 m/min i.e. at optimal welding parameters for 1 mm thick FSS. The weld is medium wide with independent grains in the centre (equiaxial WPSM) to which comparatively long oriented grains grow from both sides. There is a heat-affected zone (HAZ) with non-oriented grains. The longer oriented grains are approx. 1,3 mm long and have a cross section of 0,2×0,3 mm.

The results of tensile tests showed that at equiaxial WPSM (Figure 5A) joint brakes outside the weld or in a HAZ and has a higher tensile strength compared to epitaxial WPMS (Figure 5C), at which joint usually breaks in the centre of the weld and has a lower tensile strength.

The equiaxial WPSM is, according to the literature data, produced by individual elements in the weld pool, which act as nuclei for the grain growth. In our case this cannot be true since we have used base FSS with the same chemical composition. The formation of intermediate layer of independent grains can be attributed to the weld-pool motion and weld pool temperature gradients at the liquid/solid phase interface. It was first time experimentally found with which parameters the intermediate layer of grains in the weld centre is formed.

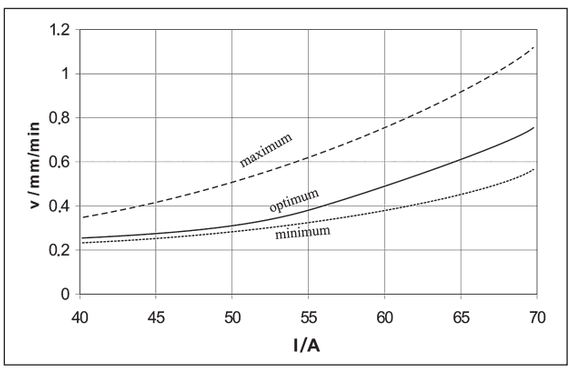

Figure 4 Optimum values of welding speed and welding current in welding of 1 mm thick FSS

Figures 5B and 5D shows four BWJ welded with 40 A (a), 50 A (b), 60 A (c) and 70 A (d) of welding current.

Figures 5B and 5D shows four BWJ welded with 40 A (a), 50 A (b), 60 A (c) and 70 A (d) of welding current. A figure schematically shows the widths of the weld (4) and HAZ (3), the grain orientation and size, the locations of fracture in tensile testing (5), the width of the intermediate layer of independent grains and the locations of this layer (1). The intermediate layer was only formed at lower welding currents (Figure 5B), where smaller quantity of molten metal was lagging behind the arc. At higher welding current, the weld pool in the weld centre was overheated i.e. the centre had a higher temperature; therefore, the conditions for formation of the independent grains in the centre were not present. Similar conditions were observed at welding with higher welding speed of 0,39 m/min (Figure 5D). The intermediate layer of grains only appeared when welding with 60 A. The reason for appearance and absence of intermediate layer of grains at welding with similar parameters could be explained with the weld pool motion.

Figure 6 shows the weld-pool motion during welding in the top plane at low and high welding speeds. A weld pool is surrounded by a solid base metal and is affected by various mechanical forces, producing the weld-pool motion. These forces are: surface tension, electromagnetic forces, forces due to filler-material droplet transfer through the arc, the welding-arc force, and forces due to welding-burner motion. The Marangoni effect describes the weld-pool motion between its surface and its bottom [21]

At higher welding speeds the weld pool is lagging behind the arc and stays overheated. The molten metal in the

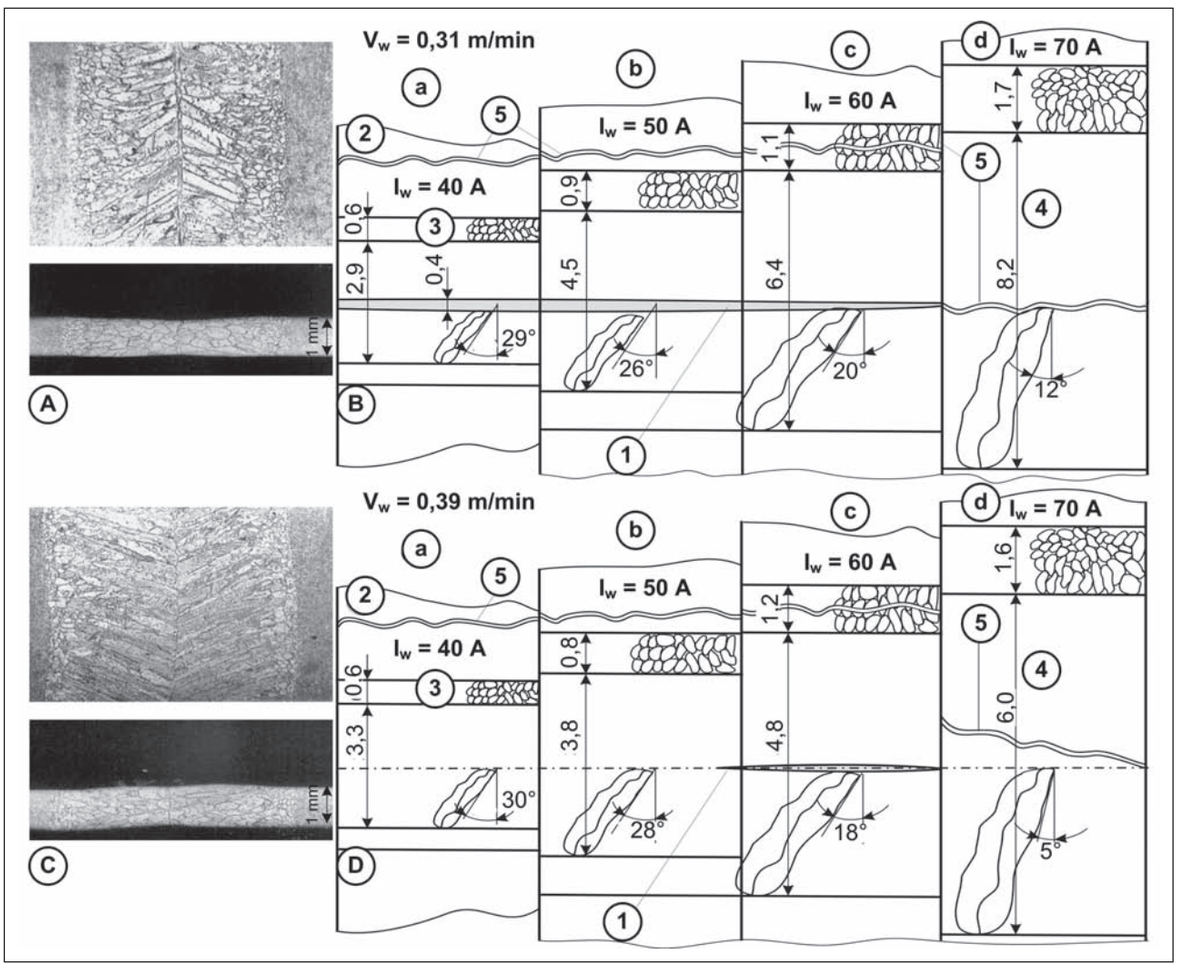

Figure 5 Top and side of view of weld macrograph (A → 40 A, 0,31 m/min, C → 50 A, 0,39 m/min) and B) and D) (4) BWJ showing widths of weld and (3) HAZ, (5) location of fracture in tensile testing, grain size and shape in weld and (1) location of intermediate layer of independent grains, at different welding currents (a-d)

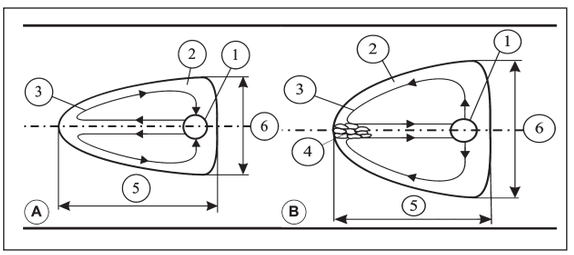

Figure 6 Schematic representation of weld-pool motion in welding of 1 mm thick FSS sheet with a) high and b) low welding speed. 1 – welding arc, 2 – weld pool, 3 - direction of weld-pool motion, 4 – intermediate layer of grains, 5 - weld-pool length, 6 – weld-pool width

weld pool moves from the centre out to the pool edge, where it transmits a portion of its thermal energy. At the weld centre the temperature is higher than at the edge, so grains grow towards the weld centre i.e. epitaxial WPSM.

At lower welding speeds a larger volume of the weld pool is obtained. Therefore it moves before the arc sideways and then downward along the edge, up to the pool bottom and then again upward to the weld-metal centre (anti clock wise). A high temperature maintained at weld pool sides slows down the grain growth from the base metal towards the centre and promotes the formation of the intermediate layer of independent grains at the weld centre due to the lower melt temperature. The weld pool starts solidifying in the weld centre before the grains from the sides reaches the weld centre i.e. equiaxial WPSM is obtained. Figure 7 shows a macrograph of a butt welded joint containing the HAZ and the intermediate layer of the independent grains. This layer of grains in the weld centre will favour strength properties of the entire welded joint.

CONCLUSIONS

Based on this study, the following conclusions may be drawn:

- For an optimum strength of welded joints from a FSS, the weld should have a layer of independent grains in its centre.
- The decisive factor in the formation of the intermediate layer of grains is the mode of weld-pool motion during welding. The latter, in turn, depends on the welding parameters.
- The optimum welding parameters for the 1 mm thick FSS sheet welded in a mixture of Ar + 5 % H_2 are the following: I = 40 – 60 A at the welding speed of 0,31 m/min and 60 A at the welding speed of 0,39 m/min.

REFERENCES

[1] S. Kou, Welding metallurgy, 2nd ed., A Wiley-Interscience publication, Hoboken, New Jersey, 2003, pp. 170 – 215.
[2] M. Pleterski, J. Tušek, L. Kosec, M. Muhič, T. Muhič, Laser repair welding of moulds with various pulse shapes, Metalurgija 46 (2010) 1, 41–44.
[3] L.A. Tarshis, J.L. Walker, J.W. Rutter, Experiments on the Solidification Structure of Alloy Castings, Metallurg. Transactions, 2 (1971), 2589 – 2597.

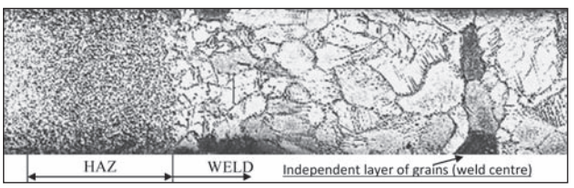

Figure 7 Macrograph of a part of BWJ with a layer of independent grains in weld centre; 1 mm thick FSS, I = 40 A, V = 0,31 m /min, U = 12 V, gas: Ar + 5 % H2

[4] B. Scholtes, E. Macherauch, Auswirkungen mechanischer Randschichtverformungen auf das Festigkeitsverhalten metallischer Werkstoffe, Zeitschrift für Metallkunde, 77 (1986) 5, 322 – 337.
[5] I. Dustin, W. Kurz, Modeling of Cooling Curves and Microstructures During Equiaxed Dendritic Solidification. Zeitschrift für Metallkunde, 77 (1986) 5, 265 – 273.
[6] J.D. Hunt, Steady State Columnar and Equiaxed Growth of Dendrites and Eutectic, Metal Science and Engineering, 65 (1984), 75 – 83,
[7] K. Easterling, Introduction to the Physical Metallurgy of Welding, Butterworths Monographs in Materials, London, 1983.
[8] J. Clarke, D.C. Weckman, H.W. Kerr, The Columnar-to-Equiaxed grain Transition in Gas Tungsten Arc Welds, 36 Ann. Conf. Metall. Of CIM, Light Metals Symposium 97, Sudbury, Ontario, 1997.
[9] O. Grong, Metallurgical Modeling of Welding, The Institute of Materials, 1997.
[10] E. Hornbogen, The Origin of Microstructures of Rapidly Solidified Alloys, Zeitschrift für Metallkunde, 77 (1986) 5, 306 – 311.
[11] S. Kou, Y. Le, Welding Parameters and Grain Structure of Weld Metal – A Thermodynamic Consideration, Metallurg. Trans. A, 19A (1988), 1075 – 1082.
[12] C. Huang, S. Kou, Partially Melted Zone in Aluminium Welds – Planar and Cellular Soldification, Welding Journal, 80 (2001), 46s – 53s.
[13] J. C. Villafuerte, E. Pardo, H. W. Kerr, The Effect of Alloy Composition and Welding Conditions on Columnar – Equiaxed Transitions in Ferritic Stainless Steel Gas – Tungsten Arc Welds, Metallurg. Transa. A, 21A (1990), 2009 – 2019.
[14] J.C. Villafuerte, H.W. Kerr, S.A. David, Mechanisms of equiaxed grain formation in ferritic stainless steel gas tungsten arc welding, Materials Science & Engineering A, 194 (1995) 2, 187 – 191.
[15] K. Witke, Bedeutung der Primärkristallisation des Schweißgutes bei Schmelzschweißverfahren, Schweißtechnik, 15 (1965) 6, 278 –279.
[16] K. Witke, Gesetzmäßigkeiten der Primärkristallisation beim Schweißen, Schweißtechnik, 16 (1966) 4, 158 –164.
[17] K. Witke, Besonderheiten der Primärkristallisation des Schweißguts, Schweißtechnik, 16 (1966) 6, 289 –292.
[18] F. Eichorn, A. Engel, Primärkristallisation beim Schmelzschweißen, Schweißen und Schneiden, 25 (1973) 11, 495 – 499.
[19] F. Markelj, J. Tušek, Algorithmic optimisation of parameters in tungsten inert gas welding of stainless steel sheet, Sci. and Technol. of Weld. and Join., 6 (2001) 6, 375-382.
[20] S. Katayama, Solidification phenomena of weld metals, Solidification cracking mechanism and cracking susceptibility (3rd Report), Welding International, 15 (2001) 8, 627 – 636.
[21] W. Middel, G. den Ouden, Additive assisted through the arc sensing during gas tungsten arc welding, Sci. and Technol. of Weld. and Join., 4 (1999) 6, 335 – 339.

Note: The responsible translator for English language is Urška Letonja, Moar.Prevajanje, Slovenia.